



Silver nanoparticles fluorescence enhancement effect for determination of nucleic acids with kaempferol–Al(III)

Yinghua Cao^{a,1}, Xia Wu^{a,*}, Minqin Wang^{b,1}

^a Key Laboratory of Colloid and Interface Chemistry (Shandong University), Ministry of Education, School of Chemistry and Chemical Engineering, Shandong University, Jinan 250100, PR China

^b College of Life Science Shandong University, Jinan 250100, PR China

ARTICLE INFO

Article history:

Received 23 January 2011

Received in revised form 16 February 2011

Accepted 12 March 2011

Available online 23 March 2011

Keywords:

Nucleic acids

Fluorescence

Kaempferol

Silver nanoparticle

Al(III)

ABSTRACT

Nucleic acids can greatly enhance fluorescence intensity of the kaempferol (Km)–Al(III) system in the presence of silver nanoparticles (AgNPs). Based on this, a novel method for the determination of nucleic acids is proposed. Under studied conditions, there are linear relationships between the extent of fluorescence enhancement and the concentration of nucleic acids in the range of 5.0×10^{-9} to 2.0×10^{-6} g mL⁻¹ for fish sperm DNA (fsDNA), 7.0×10^{-9} to 2.0×10^{-6} g mL⁻¹ for salmon sperm DNA (smDNA) and 2.0×10^{-8} to 3.0×10^{-6} g mL⁻¹ for yeast RNA (yRNA), and their detection limits are 2.5×10^{-9} g mL⁻¹, 3.2×10^{-9} g mL⁻¹ and 7.3×10^{-9} g mL⁻¹, respectively. Samples were satisfactorily determined. And the system of Km–Al(III)–AgNPs was used as a fluorescence staining reagent for sensitive DNA detection by DNA pattern of agarose gel electrophoresis analysis. The results indicate that the fluorescence enhancement should be attributed to the formation of Km–Al(III)–AgNPs–nucleic acids aggregations through electrostatic attraction and adsorption bridging action of Al(III) and the surface-enhanced fluorescence effect of AgNPs.

© 2011 Elsevier B.V. All rights reserved.

1. Introduction

Nucleic acid is the basic material of life and its quantitative determination is important in life analysis. Fluorometric analysis is one of the most important technologies for nucleic acid determination due to its advantages such as high sensitivity, good selectivity and simplicity. Studies of nucleic acid through fluorometric analysis are an active field for chemical and biochemical research [1–5]. The key to fluorometric analysis is the spectrophotometric probe. Presently, the exploration for a superior fluorescence probe is one of the hottest topics in the bioassay field [6].

Currently noble metal nanoparticles such as silver nanoparticles (AgNPs) and gold nanoparticles have been given much attention because of their unique physical and chemical characteristics [7–12]. Si et al. [13–15] reported that the fluorescence intensity of organic dyes can be enhanced by AgNPs because of its surface-enhanced fluorescence (SEF) effect. Additionally, AgNPs have high affinity for nucleic acid [16]. In this work, AgNPs were selected as a new fluorescence signal enhancement reagent for kaempferol

as the fluorescent probe for quantitative determination of nucleic acids.

Kaempferol (Km) is a kind of flavonoid (Fig. 1), which is a natural substance and universally present in fruits, vegetables and crops. Flavonoids have many physiological activities such as being an antioxidant, cardiovascular disease and anticancer reagent [17–19]. Km–metal or non-metal has been widely studied [20–23], but there are poor studies with Km–metal–Nucleic acids systems. Zhang et al. [24] studied the interaction between Km–Eu³⁺ complex and DNA using Neutral Red dye as a fluorescent probe.

In this study, the SEF effect of AgNPs was used to find a novel fluorescence probe of Km–Al(III)–AgNPs and developed a new stable and sensitive method for the trace determination of nucleic acids. Experiments showed that the enhanced fluorescence intensity was in proportion to the concentrations of nucleic acids. The interaction mechanism of the system was also studied by transmission electronic microscopy (TEM), resonance light scattering (RLS), circular dichroism spectra (CD), UV spectrometry and fluorometric method.

2. Experimental

2.1. Chemicals

Stock solutions of nucleic acids (100 µg mL⁻¹) were prepared by dissolving commercial fsDNA (Sigma), smDNA (Shanghai

* Corresponding author at: Shandong University, School of Chemistry and Chemical Engineering, Shanda Nanlu 27#, Jinan, Shandong Province 250100, PR China. Tel.: +86 531 88365459; fax: +86 531 88564464.

E-mail address: wux@sdu.edu.cn (X. Wu).

¹ Co-author of first.

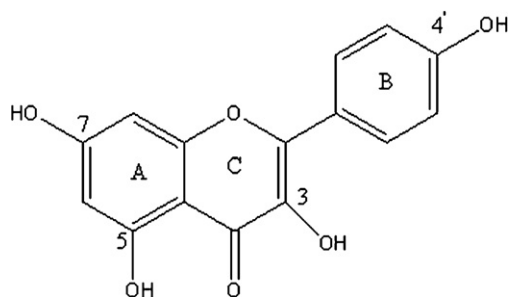


Fig. 1. Chemical structure of Km.

Qiuzhiyou Co., China) and yRNA (Beijing Baitai Co., China) in 0.05 mol L^{-1} sodium chloride solutions. AgNPs preparation [25]: a stock solution of silver nanoparticles ($2.0 \times 10^{-4} \text{ g mL}^{-1}$ calculated by the silver ion added) was prepared by dissolving 15.8 mg of AgNO_3 in 40 mL of $0.22 \mu\text{m}$ -filtered ultra pure water ($18.25 \text{ M}\Omega \text{ cm}^{-1}$), then 2.0 mL sodium citrate (1%, w/v) was slowly added into the AgNO_3 solution by heating at 86°C with stirring for 30 min. The solution color changed gradually from colorless to olivine. Finally the solution was diluted to 50 mL with ultra pure water. A standard stock solution ($1.0 \times 10^{-3} \text{ mol L}^{-1}$) of Km purchased from Shanghai Ronghe Co., China was prepared by dissolving 14.3 mg of Km and diluting it to 50 mL with absolute ethyl alcohol. The prepared solutions were stored at $0\text{--}4^\circ\text{C}$. A stock solution ($2.2 \times 10^{-3} \text{ mol L}^{-1}$) of aluminum chloride purchased from Chemical Co. of China, Beijing, was prepared with ultra pure water. A Britton–Robison (BR, 0.04 mol L^{-1}) buffer solution was prepared containing 380 μL of glacial acetic acid (99.5%), 460 μL of orthophosphoric acid (85%), and 112.2 mg of boric acid in 500 mL solution. The pH range, from 3.84 to 7.03, was adjusted with 0.2 mol L^{-1} sodium hydroxide. All the chemicals used were of analytical reagent grade and ultra pure water was used throughout.

2.2. Apparatus

The fluorescence and RLS measurements were performed with a LS-55 spectrofluorimeter (Perkin Elmer, USA) in a $1 \text{ cm} \times 1 \text{ cm}$ quartz cuvette. All CD spectra were collected by a J-810S Circular Dichroism Spectrometer (JASCO, Japan). All absorption spectra were measured by a U-4100 spectrophotometer (Hitachi, Japan). TEM images were obtained by a JEM-100 CXII Transmission Electron Microscope (JEOL, Japan). All pH measurements were made with a Leici pH-3C acidity meter (Jingke, Shanghai). Agarose gel electrophoresis was used by horizontal gel electrophoresis apparatus (DYY-6C, Beijing Liuyi instrument factory, China). λDNA separation pattern was analyzed with a syngene fluorescence gel imaging system (Syngene, USA).

2.3. Procedure

The solutions were added to a 10 mL colorimetric tube in the following order: BR, Al(III), AgNPs, Km and nucleic acids. The mixture was diluted to 5 mL with ultra pure water. The fluorescence intensity at 485 nm with an excitation wavelength of 260 nm was recorded and applied to the quantitative analysis of nucleic acids. Slit widths for both excitation and emission were set to 10 nm with a scan speed of 600 nm/min. The enhanced fluorescence intensity of Km–Al(III)–AgNPs–nucleic acids system is $\Delta I_f = I_f - I_0$, where I_f and I_0 were the fluorescence intensities of the systems with and without nucleic acids.

2.4. Agarose gel electrophoresis protocol

Prior to gel casting, 1 g dried low temperature agarose gel was dissolved in 100 mL TAE buffer ($1 \times \text{pH } 8.3$ Tris–acetate–EDTA buffer) by being heated in a microwave for 2–4 min and was then poured into a $18 \text{ cm} \times 18 \text{ cm}$ glass mold, which was fitted with a well-forming comb [26]. The Conventional $\lambda\text{DNA}/\text{HindIII} + \text{EcoRI}$ Digest Markers were used as DNA samples in the experiment [26]. The total 20 μL DNA mixture containing 6 μL λDNA samples (1 μL , 0.5 μg λDNA marker + 1 μL of $6 \times \text{DNA Loading Dye}$ + 4 μL of deionized water) and 14 μL Km–Al(III) or Km–Al(III)–AgNPs (Km: $5.0 \times 10^{-5} \text{ mol L}^{-1}$; AgNPs: $3.0 \times 10^{-6} \text{ g mL}^{-1}$; Al(III): $5.0 \times 10^{-4} \text{ mol L}^{-1}$; BR (pH 5.80): $8.0 \times 10^{-2} \text{ mol L}^{-1}$) were loaded in each sample well. $1 \times \text{TAE}$ electrophoresis buffer was added into a horizontal electrophoresis apparatus until the buffer just covered the agarose gel. Electrophoresis was at 70 V for 30–60 min at room temperature, depending on the desired separation. Then the gel was placed on a UV light box. A picture of the fluorescence of Km–Al(III)– λDNA or Km–Al(III)–AgNPs– λDNA , and a λDNA separation pattern (the time of exposure was 360 ms) was analyzed with a syngene gel imaging system.

3. Results and discussions

3.1. Fluorescence spectra

Fig. 2 displays the fluorescence spectra of the system. As can be seen in Fig. 2, the fluorescence intensities of Km, Km–Al(III), Km–Al(III)–AgNPs are weak. After the addition of fsDNA, the fluorescence intensities are enhanced, especially in the presence of AgNPs. The same phenomena were observed when smDNA and yRNA was added to the systems instead of fsDNA (data not shown). It is suggested that AgNPs plays a key role in fluorescence enhancement. From the fluorescence spectra, it also can be seen that the systems have an emission peak at 485 nm (Fig. 2b), and three excitation peaks at 260 nm, 362 nm and 426 nm (Fig. 2a), corresponding to the absorption bands of Km, respectively. It is apparent that the extent of fluorescence enhancement under the excitation of 260 nm is highest. Therefore, the excitation peak of 260 nm was selected for further study.

3.2. The effect of pH and the selection of buffer solution

Fig. 3 shows the effect of pH on the fluorescence intensity of the system. It can be seen that when the pH is in the range of 4.95–6.10, the ΔI_f of the system reaches the maximum. When pH is higher than 6.10, the hydration of Al(III) results in the formation of soluble polynuclear forms called hydroxo complexes, polycations or hydroxo polymers which is not conducive to the chelating between Al(III) and Km. A pH of 5.80 was selected for further research. The effect of different buffer solutions (such as Na_2HPO_4 –citric acid, HMTA–HCl, Tris–HCl, citric acid–sodium citrate and BR) on this system were also studied at the same pH ($\text{pH } 5.80 \pm 0.05$). Only in the BR buffer solution, did the fluorescence enhancement of the Km–Al(III)–AgNPs–fsDNA system appear. 0.4 mL of BR (0.04 mol L^{-1} , pH 5.80) was the most suitable buffer.

3.3. Effect of Km concentration and Al(III) concentration

Effect of Km concentration and Al(III) concentration on the fluorescence intensity is shown in Fig. 4. When the concentration ratio ($C_{\text{Al(III)}}:C_{\text{Km}}$) is in the range of 8–20, the ΔI_f value reached the maximum and remained constant. It is speculated that when the ratio of $C_{\text{Al(III)}}$ and C_{Km} is lower than 8, the strong interaction between Km and Al(III) hinders the formation of the

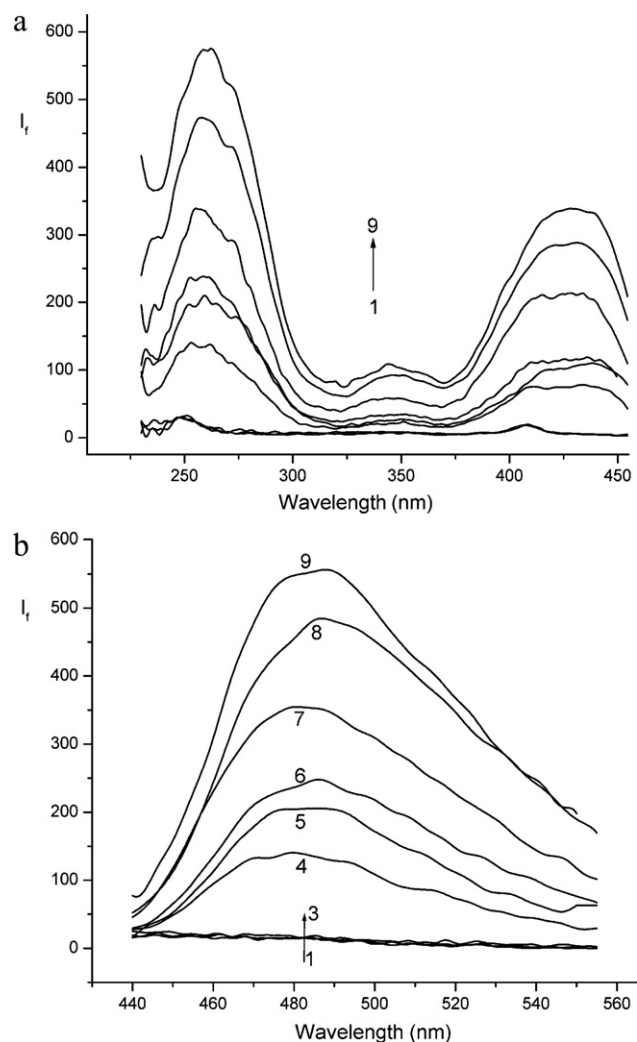


Fig. 2. Fluorescence spectra. (a) Excitation spectra ($\lambda_{em} = 485$ nm), (b) emission spectra ($\lambda_{ex} = 260$ nm). 1. Km, 2. Km–Al(III), 3. Km–AgNPs–Al(III), 4. Km–AgNPs–fsDNA, 5. Km–fsDNA, 6. Km–Al(III)–AgNPs–yRNA, 7. Km–Al(III)–fsDNA, 8. Km–Al(III)–AgNPs–smDNA, and 9. Km–Al(III)–AgNPs–fsDNA. Conditions: Km: 2.0×10^{-6} mol L $^{-1}$; Al(III): 2.0×10^{-5} mol L $^{-1}$; AgNPs: 1.2×10^{-7} g mL $^{-1}$; fsDNA: 1.0×10^{-6} g mL $^{-1}$; smDNA: 1.0×10^{-6} g mL $^{-1}$; yRNA: 1.0×10^{-6} g mL $^{-1}$; BR: 3.2×10^{-3} mol L $^{-1}$ (pH 5.80).

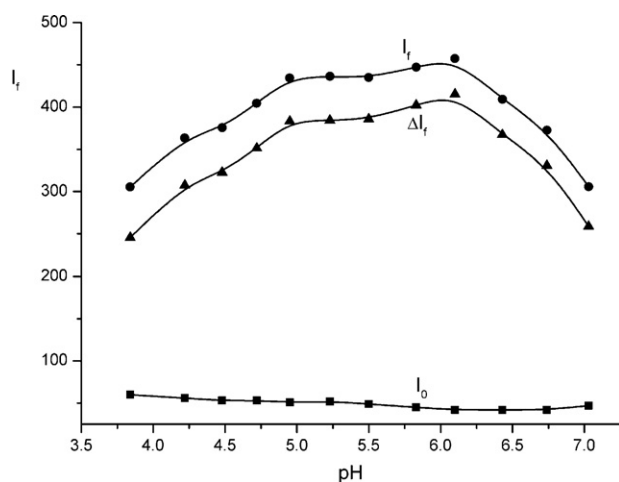


Fig. 3. Effect of pH. Conditions: Km: 2.0×10^{-6} mol L $^{-1}$; Al(III): 2.0×10^{-5} mol L $^{-1}$; AgNPs: 1.2×10^{-7} g mL $^{-1}$; fsDNA: 1.0×10^{-6} g mL $^{-1}$.

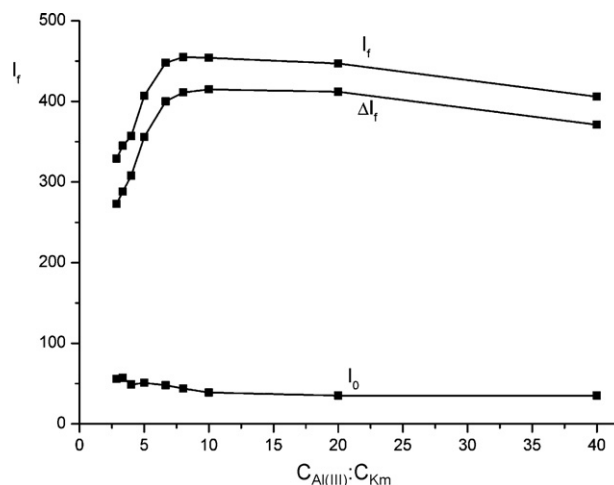


Fig. 4. Effect of Km concentration and Al(III) concentration. Conditions: Al(III): 2.0×10^{-5} g mL $^{-1}$; AgNPs: 1.2×10^{-7} g mL $^{-1}$; fsDNA: 1.0×10^{-6} g mL $^{-1}$; BR: 3.2×10^{-3} mol L $^{-1}$ (pH 5.80).

complex of the Km–Al(III)–fsDNA. When the proportion of Al(III) increases ($C_{Al(III)}:C_{Km} > 20$), the hydration of Al(III) is strengthened, which results in the adsorption bridging action of Al(III) to fsDNA weakening. So $C_{Al(III)}:C_{Km} = 10$ (Al(III): 2.0×10^{-5} mol L $^{-1}$, Km: 2.0×10^{-6} mol L $^{-1}$) was used for further research.

3.4. Effect of AgNPs concentration

The effect of AgNPs concentration on the fluorescence intensity of the system is shown in Fig. 5. It is found that the AgNPs concentration has a large effect not only on I_f , but also on I_0 . It can be seen that when the AgNPs concentration is 1.2×10^{-7} g mL $^{-1}$, the fluorescence enhancement is the best. So 1.2×10^{-7} g mL $^{-1}$ AgNPs was chosen for further research.

3.5. The addition order and stability of this system

Experiments showed the addition order had a certain influence on the ΔI_f of the system. The best addition order was found to be buffer, Km, Al(III), AgNPs and nucleic acid.

Under studied conditions, the effect of time on the fluorescence intensity was studied. The result showed that the increased flu-

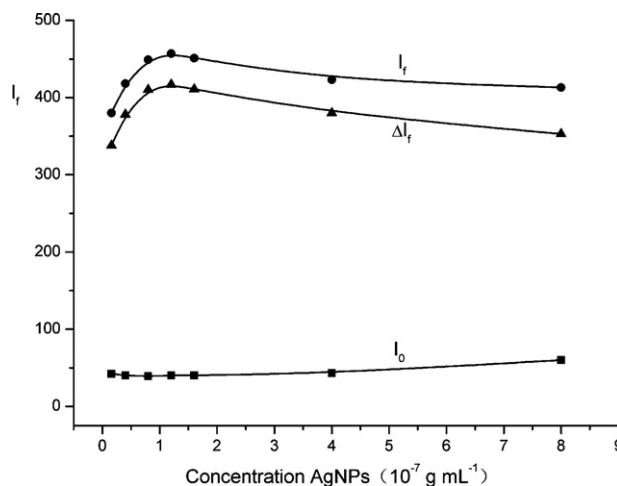


Fig. 5. Effect of the concentration of AgNPs. Conditions: Km: 2.0×10^{-6} mol L $^{-1}$; Al(III): 2.0×10^{-5} mol L $^{-1}$; fsDNA: 1.0×10^{-6} g mL $^{-1}$; BR: 3.2×10^{-3} mol L $^{-1}$ (pH 5.80).

Table 1
Interference from foreign substances.

Foreign substance	Concentration coexisting (10^{-6} mol L $^{-1}$)	Change of I_f (%)
Na $^{+}$, Cl $^{-}$	5.0	−3.9
NH $_4^{+}$, Cl $^{-}$	3.0	−4.1
Mg $^{2+}$, SO $_4^{2-}$	4.0	−4.1
Zn $^{2+}$, Cl $^{-}$	3.0	−5.9
Fe $^{3+}$, SO $_4^{2-}$	0.01	−5.3
Ca $^{2+}$, Cl $^{-}$	5.0	+3.0
Na $^{+}$, CO $_3^{2-}$	50	−4.9
K $^{+}$, Cl $^{-}$	50	−4.0
AMP	1.4	−5.3
TMP	10	−3.9
CMP	5.0	+3.6
GMP	0.8	−4.6
UMP	8.0	+4.9
L-ASP	50	−3.4
His	50	−3.4
BSA	3.0 μ g mL $^{-1}$	−4.8

Conditions: Km: 2.0×10^{-6} mol L $^{-1}$; Al(III): 2.0×10^{-5} mol L $^{-1}$; AgNPs: 1.2×10^{-7} g mL $^{-1}$; fsDNA: 3.0×10^{-7} g mL $^{-1}$; BR: 3.2×10^{-3} mol L $^{-1}$ (pH 5.80).

orescence intensity immediately reaches a maximum after all the reagents are added. And it can remain stable for over 1 h. Therefore, this system exhibits rapid reaction and good stability.

3.6. Effect of foreign substances

Under studied conditions, various coexisting substances in the organism including common metal ions, bases, amino acids and protein were examined for interference. Table 1 shows that most of them except Fe $^{3+}$ have no or little effect on the determination of nucleic acid, under the permission of $\pm 5\%$ relative error.

4. Analytical applications

4.1. The calibration graph and detection limits

Under studied conditions defined here, the calibration curves for fsDNA, smDNA and yRNA were obtained and the analytical parameters are shown in Table 2. It shows that there is a good linear relationship between ΔI_f and the concentrations of nucleic acids. And their limit of detection is down to 10^{-9} g mL $^{-1}$. The relative standard deviations calculated from nine determinations at 3.0×10^{-7} g mL $^{-1}$ fsDNA, smDNA and yRNA are 1.0%, 0.94% and 1.6%, respectively. This indicates that the system has good reproducibility. The analytical parameters with the excitation wavelength at 426 nm for comparison are also displayed in Table 2. The result shows that when the excitation wavelength is at 260 nm, the sensitivity of the method for DNA determination is better.

To further validate the action of AgNPs in improving the fluorescence determination method of trace nucleic acids, the sensitivity and linear range were compared in two systems of Km–Al(III)–fsDNA with and without AgNPs. The conditions of the Km–Al(III)–fsDNA system for nucleic acids determination were optimized. Under its studied conditions, a linear calibration graph was obtained over the range from 3.0×10^{-8} g mL $^{-1}$ to 3.0×10^{-6} g mL $^{-1}$ with a detection limit of 1.4×10^{-8} g mL $^{-1}$ for fsDNA. The system of Km–Al(III)–fsDNA with AgNPs provides a wider linear range and a lower detection limit for nucleic acid determination. It is proved that the system of Km–Al(III)–AgNPs–fsDNA shows higher sensitivity than that of the Km–Al(III)–fsDNA system.

4.2. Determination of a sample

The standard addition method was used for the determination of *Arabidopsis thaliana* DNA in the sample. The content of *A. thaliana* DNA in the sample was 583 ng μ L $^{-1}$, which was obtained by using a Biophotometer (Eppendorf Co.). The sample was diluted 10,000-fold with water and determined by the proposed method. The average of five measurements is 581 ng μ L $^{-1}$ and the relative standard deviation is 2.8% ($n=5$). Hence, the proposed method is suitable for the determination of trace amount of nucleic acids in this sample.

4.3. Agarose gel electrophoresis analysis

Fig. 6 shows the electrophoresis pattern of the λ DNA size marker. The majority of λ DNA fragments pattern clearly appeared just after Km–Al(III)–AgNPs were added on the surface of the agarose gel (Fig. 6A(b)). In Fig. 6A(a), only the size of 21,226 bp DNA fragments pattern can be discerned. After 4 min of Km–Al(III)–AgNPs addition, the smallest size of λ DNA fragments pattern (564 bp) distinctly emerged. Although most of the λ DNA fragments pattern by Km–Al(III) staining appeared, they were dim (Fig. 6B). After 5 min, λ DNA fragments patterns of Km–Al(III)–AgNPs treatment were clearest. The fluorescence intensity of λ DNA, with combination of Km–Al(III), was enhanced but was not higher than Km–Al(III)–AgNPs systems (Fig. 6C). From Fig. 6, it can be seen that the AgNPs can directly enhance the sensitivity of DNA detection by DNA pattern of agarose gel electrophoresis analysis. The results provide a convenient, reliable method which does not exist in other DNA detection facilities.

5. Interaction mechanism

5.1. The interaction between Km, Al(III) and fsDNA

The UV absorption spectra of the system of Km and Al(III) with increasing concentration of fsDNA was obtained. Km absorbed with a maximum at 360 nm (band I) and 260 nm (band II). Band I corresponds to ring B (cinnamoyl system) and band II to ring A (benzoyl system) (Fig. 1) [27]. After adding fsDNA to the system of Km–Al(III), a new peak emerged at 413 nm and there were three isosbestic points at 270 nm, 385 nm and 474 nm (Fig. 7), which suggests that Al(III) has bonded to 3-hydroxyl and 4-carbonyl of ring C [28]. In this condition, the concentration of Al(III) is far greater than that of Km. It is believed that except for the chelating between Al(III) with Km, Al(III) can still combine with phosphate groups in nucleic acid through electrostatic interaction [29]. And by the adsorption bridging action of Al(III), the ternary complex of Km–Al(III)–fsDNA is formed. At the same time, fsDNA provides a hydrophobic environment for Al(III) and weakens the hydration of Al(III) [30].

5.2. The formation of the aggregates of Km–Al(III)–AgNPs–fsDNA

According to the RLS theory [31,32], the intensity of a RLS should sensitively depend on the size of the aggregate and the extent of the electronic coupling among chromophores. As shown in Fig. 8, the RLS intensity of Km–Al(III) is low, whereas it is enhanced in the present of fsDNA, which indicates the formation of the ternary complex of Km–Al(III)–fsDNA. And when AgNPs are added into the Km–Al(III)–fsDNA complex, the RLS intensity is greatly enhanced. It is concluded that larger aggregates of Km–Al(III)–AgNPs–fsDNA are formed. Previous work [33] confirm that electrostatic interaction exists between AgNPs–fsDNA and Al(III).

The TEM images of AgNPs (a), AgNPs–fsDNA (b) and Km–Al(III)–AgNPs–fsDNA (c) are shown in Fig. 9. From Fig. 9a,

Table 2
Analytical parameters of this method.

Excitation wavelength (nm)	DNA	Linear range (g mL ⁻¹)	r ^a	Linear regression equation (g mL ⁻¹)	LOD ^b (g mL ⁻¹)
260	fsDNA	5.0 × 10 ⁻⁹ to 2.0 × 10 ⁻⁶	0.998	ΔI _f = 15.2 + 4.18 × 10 ⁸ C	2.5 × 10 ⁻⁹
	smDNA	7.0 × 10 ⁻⁹ to 2.0 × 10 ⁻⁶	0.997	ΔI _f = 5.82 + 3.68 × 10 ⁸ C	3.2 × 10 ⁻⁹
	yRNA	2.0 × 10 ⁻⁸ to 3.0 × 10 ⁻⁶	0.996	ΔI _f = 2.40 + 2.82 × 10 ⁸ C	7.3 × 10 ⁻⁹
426	fsDNA	7.0 × 10 ⁻⁸ to 3.0 × 10 ⁻⁶	0.998	ΔI _f = 10.1 + 2.75 × 10 ⁸ C	9.0 × 10 ⁻⁹

^a Correlation coefficient.
^b Limit of detection.

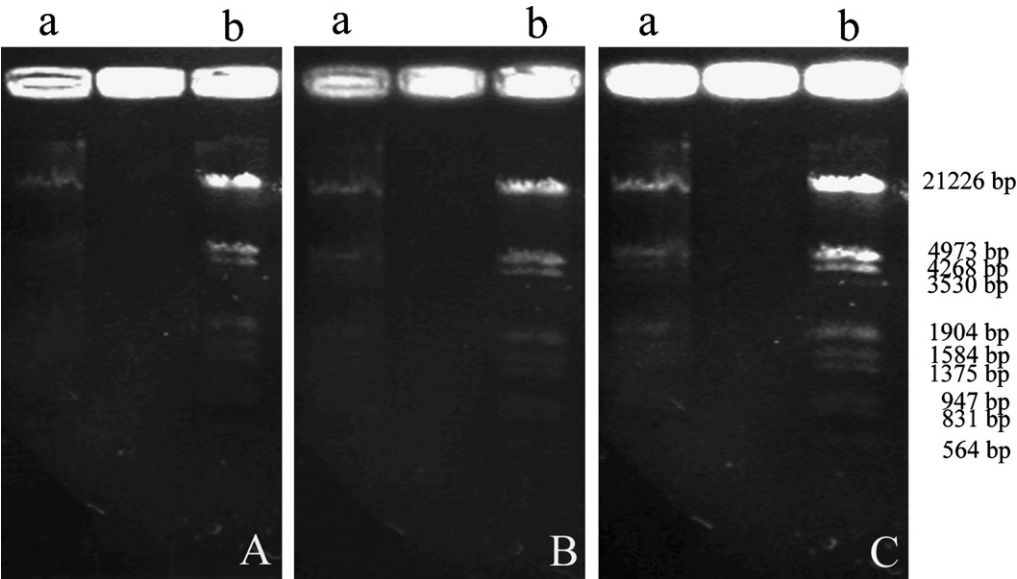


Fig. 6. Electrophoresis pattern of the λDNA size marker cut with *Hind*III+*Eco*RI. Km–Al(III)–λDNA/Km–Al(III)–AgNPs–λDNA treated for 0 min (A); 4 min (B); 5 min (C). (a) Km–Al(III)–λDNA; (b) Km–Al(III)–AgNPs–λDNA. 21,226 bp, 4973 bp and 564 bp express the size of DNA fragments. Conditions: Km: 5.0 × 10⁻⁵ mol L⁻¹; Al(III): 5.0 × 10⁻⁴ mol L⁻¹; AgNPs: 3.0 × 10⁻⁶ g mL⁻¹; BR: 8.0 × 10⁻² mol L⁻¹ (pH 5.80).

it can be seen that AgNPs are spherical in shape with a diameter of 10–15 nm, and they are well dispersed. When fsDNA was added to AgNPs solution, larger aggregates were formed and their diameter was about 100 nm (Fig. 9b). In the system of Km–Al(III)–AgNPs–fsDNA, it can be seen that nanoparticles congregate and form large agglomerations with a diameter of about

600 nm (Fig. 9c). The conclusions are consistent with that received from RLS.

5.3. Study on the conformation of fsDNA

The UV range CD-spectra is an effective mean to monitor the conformational transition of nucleic acids [34,35]. As shown in the CD spectrum of fsDNA (Fig. 10), the positive cotton effect at 278 nm

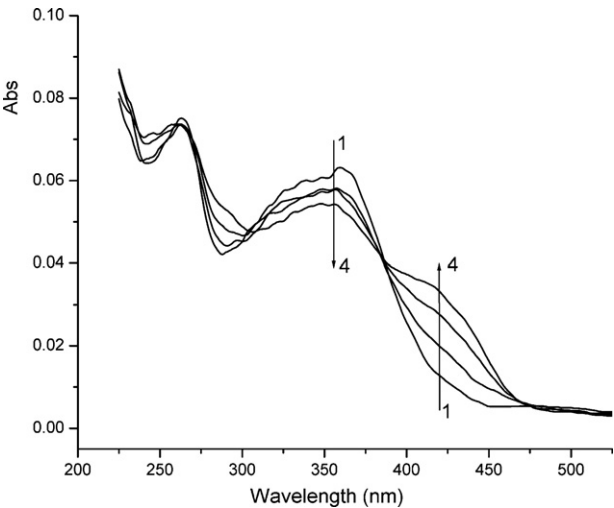


Fig. 7. Absorption spectra of Km–Al(III)–fsDNA. 1. Km–Al(III) (vs. buffer), and 2–4. Km–Al(III)–fsDNA (vs. fsDNA). Conditions: Km: 6.0 × 10⁻⁶ mol L⁻¹; Al(III): 6.0 × 10⁻⁵ mol L⁻¹; fsDNA: 0, 3.0 × 10⁻⁶, 1.0 × 10⁻⁵, 2.0 × 10⁻⁵ g mL⁻¹ corresponding to the curves from 1 to 4, respectively. BR: 3.2 × 10⁻³ mol L⁻¹ (pH 5.80).

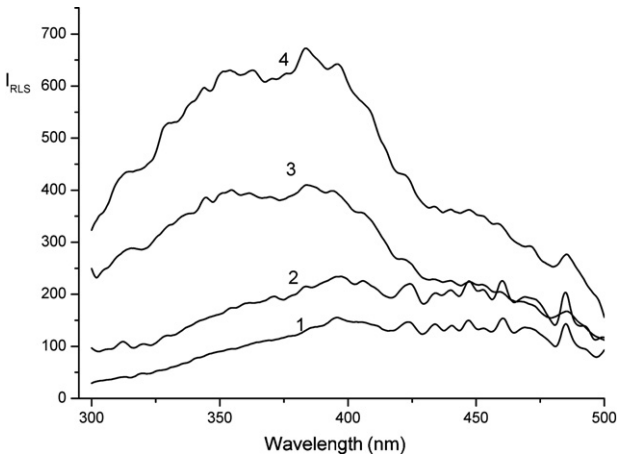


Fig. 8. Resonance light scattering spectra. 1. Km–Al(III), 2. Km–Al(III)–fsDNA, 3. Km–Al(III)–AgNPs, 4. Km–Al(III)–AgNPs–fsDNA. Conditions: Km: 2.0 × 10⁻⁶ mol L⁻¹; Al(III): 2.0 × 10⁻⁵ mol L⁻¹; AgNPs: 1.2 × 10⁻⁷ g mL⁻¹; fsDNA: 1.0 × 10⁻⁶ g mL⁻¹; BR: 3.2 × 10⁻³ mol L⁻¹ (pH 5.80).

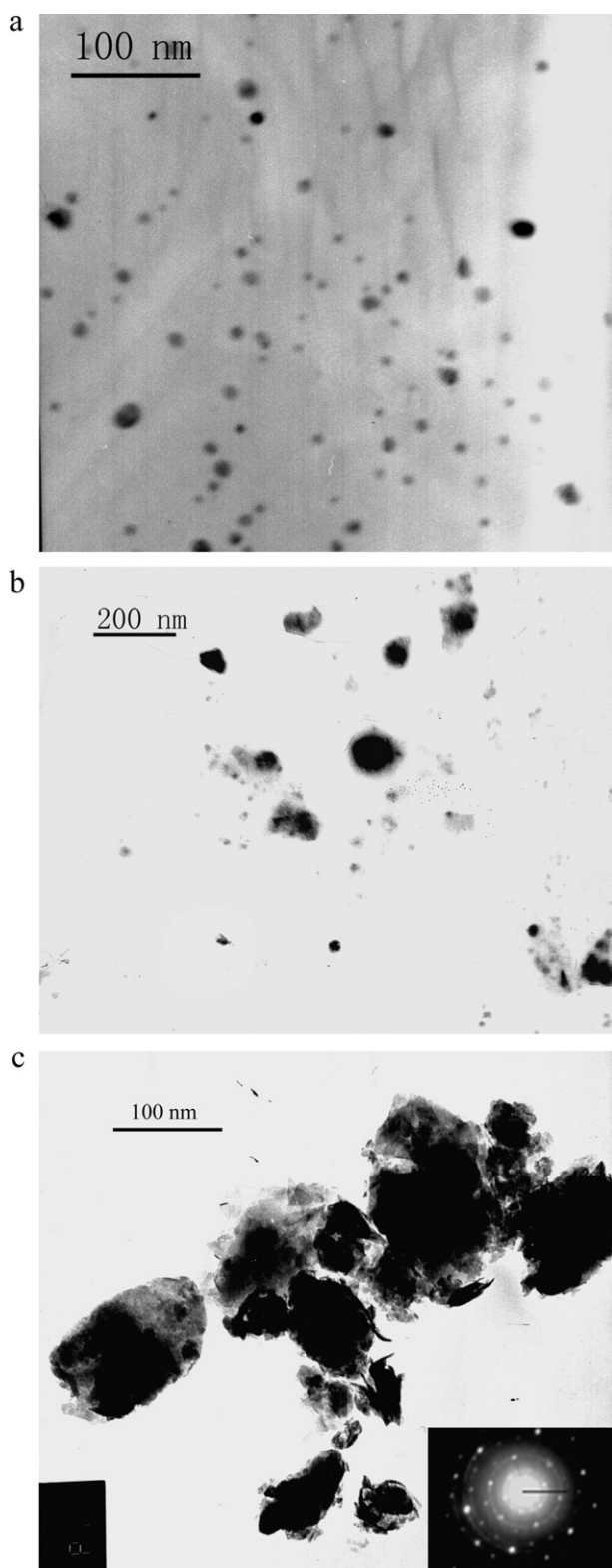


Fig. 9. Transmission electronic microscopy images. (a) AgNPs, (b) AgNPs-fsDNA, and (c) Km-Al(III)-AgNPs-fsDNA. Conditions: Km: $2.0 \times 10^{-6} \text{ mol L}^{-1}$; Al(III): $2.0 \times 10^{-5} \text{ mol L}^{-1}$; AgNPs: $1.2 \times 10^{-6} \text{ g mL}^{-1}$; fsDNA: $1.0 \times 10^{-6} \text{ g mL}^{-1}$; BR: $3.2 \times 10^{-3} \text{ mol L}^{-1}$ (pH 5.80).

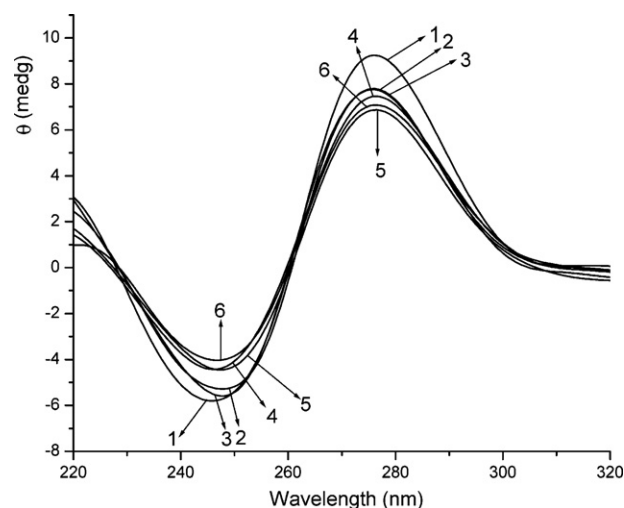


Fig. 10. CD spectra of the system. 1. AgNPs-fsDNA, 2. Km-fsDNA, 3. fsDNA, 4. Km-Al(III)-fsDNA, 5. Al(III)-fsDNA, and 6. Km-Al(III)-AgNPs-fsDNA. Conditions: Km: $2.0 \times 10^{-6} \text{ mol L}^{-1}$; Al(III): $2.0 \times 10^{-5} \text{ mol L}^{-1}$; AgNPs: $1.2 \times 10^{-7} \text{ g mL}^{-1}$; fsDNA: $5.0 \times 10^{-5} \text{ g mL}^{-1}$; BR: $3.2 \times 10^{-3} \text{ mol L}^{-1}$ (pH 5.80).

is related to base stacking, and the negative cotton effect at 246 nm is related to helicity. After adding AgNPs to the fsDNA solution, the positive peak increases more obviously than the negative peaks. Km has little effect on the fsDNA CD spectrum, whereas, the addition of Al(III) leads to a decrease of both its positive peak and negative peak. Moreover, the effect of Al(III) on the CD spectrum of fsDNA is similar to that of Km-Al(III)-AgNPs. It is known [16] that AgNPs have interaction with the nucleobases of fsDNA, which induces the change of nonplanar and tilted orientations of fsDNA bases. So it is speculated that changes of fsDNA conformation are attributed to the synergistic effect of Km, Al(III), AgNPs and fsDNA. Also, the conformation of fsDNA is mainly influenced by the electrostatic interaction between Al(III) and phosphate groups in fsDNA.

5.4. SEF effect of AgNPs

AgNPs have a SEF effect. The fluorescence enhancement depends on the coupling of excited fluorophores with the surface plasmon resonance present in metal nanoparticles. The phenomenon of surface plasmon-coupled emission (SPCE) occurs for fluorophores 20–250 nm from the metal surface [36,37].

As Fig. 2b shows, the fluorescence intensity of Km-Al(III)-AgNPs is weak. Upon adding fsDNA to the Km-Al(III)-AgNPs system, the fluorescence intensity is strongly enhanced. It is known that DNA has a large aspect ratio (length/diameter). According to the SEF mechanism, it is concluded that an optimum distance was obtained between Km-Al(III) and the surface of the AgNPs, resulting from the effect of fsDNA. As a result, the complexes of Km-Al(III) are in the surface local field of AgNPs in the presence of nucleic acids and the surface plasmon resonance effect results in fluorescence enhancement. Finally, the sensitivity for nucleic acid determination is improved. More detail investigations on the fluorescence enhancement mechanism of the system are in progress.

6. Conclusions

In this study, it was found that the further fluorescence enhancement of Km-Al(III) by nucleic acids occurs in the presence of AgNPs. Based on this, a rapid and sensitive method for the determination of nucleic acids was established. Under studied conditions, the extent of fluorescence enhancement is in proportion to the concentration of nucleic acids (e.g. fsDNA, smDNA and yRNA), with detection

limits at the 10^{-9} g mL $^{-1}$ level. The results for the determination of *A. thaliana* DNA were satisfactory. AgNPs can directly enhance the sensitivity of DNA detection by DNA pattern of agarose gel electrophoresis analysis. The investigation of the mechanism indicated that nucleic acids can promote the chelating between Km and Al(III), and with the addition of AgNPs, Km–Al(III)–AgNPs–fsDNA aggregates were formed. In addition, the effect of fsDNA resulted in an optimum distance between Km–Al(III) and the surface of AgNPs.

Acknowledgments

This work is supported by Natural Science Foundations of China (20833010) and Shandong Province (Z2008B04). Thanks to Dr. Edward C. Mignot, Shandong University, for linguistic advice.

References

- [1] C.B. Ma, Z.W. Tang, X.Q. Huo, X.H. Yang, W. Li, W.H. Tan, *Talanta* 76 (2008) 458–461.
- [2] H.P. Zhou, X. Wu, W. Xu, J.H. Yang, Q.X. Yang, *J. Fluoresc.* 24 (2010) 843–850.
- [3] M. Massey, U.J. Krull, *Anal. Bioanal. Chem.* 398 (2010) 1605–1614.
- [4] C.X. Liu, L. Wang, W. Jiang, *Talanta* 81 (2010) 597–601.
- [5] L. Li, J.H. Yang, X. Wu, C.X. Sun, G.J. Zhou, *Talanta* 59 (2003) 81–87.
- [6] Y.X. Wang, J.S. Li, H. Wang, J.Y. Jin, J.H. Liu, K.M. Wang, W.H. Tan, R.H. Yang, *Anal. Chem.* 82 (2010) 6607–6612.
- [7] C. Deeb, R. Bachelot, J. Plain, A.-L. Baudrion, S. Jradi, A. Bouhelier, O. Soppera, P.K. Jain, L.B. Huang, C. Ecoffet, L. Balan, P. Royer, *Nano Lett.* 4 (2010) 4579–4586.
- [8] J. Zhang, Y. Fu, M.H. Chowdhury, J.R. Lakowicz, *Nano Lett.* 7 (2007) 2101–2107.
- [9] A. Shkilnyy, M. Souce, P. Dubois, F. Warmont, M.L. Saboungi, I. Chourpa, *Analyst* 134 (2009) 1868–1872.
- [10] H.M. Bok, K.L. Shuford, S. Kim, S.K. Kim, S. Park, *Nano Lett.* 8 (2008) 2265–2270.
- [11] X.X. Han, Y. Kitahama, T. Itoh, C.X. Wang, B. Zhao, Y. Ozaki, *Anal. Chem.* 81 (2009) 3350–3355.
- [12] A.J. Haes, W.P. Hall, L. Chang, W.L. Klein, R.P. Van Duyne, *Nano Lett.* 4 (2004) 1029–1034.
- [13] M.Z. Si, R.G. Wu, P.X. Zhang, *Chin. J. Chem. Phys.* 15 (2002) 346–350.
- [14] W. Mao, Y. Li, K.Q. Zhou, Q. Zhou, J.W. Zheng, *Chin. J. Spectrosc. Lab.* 26 (2009) 885–887.
- [15] J. Lukomska, J. Malicka, I. Gryczynski, Z. Leonenko, J.R. Lakowicz, *Substr. Biopolym.* 77 (2005) 31–37.
- [16] J.H. Zheng, X. Wu, M.Q. Wang, D.H. Ran, W. Xu, J.H. Yang, *Talanta* 74 (2008) 526–532.
- [17] G. Rusak, H.O. Gutzeit, J. Ludwig-Mueller, *Nutr. Res.* 25 (2005) 143–155.
- [18] O.K. Chun, S.J. Chung, K.J. Claycombe, W.O. Song, *J. Nutr.* 138 (2008) 753–760.
- [19] J.W. Kang, J.H. Kim, K. Song, S.H. Kim, J.-H. Yoon, K.-S. Kim, *Phytother. Res.* 24 (2009) 77–82.
- [20] P.C.H. Hollman, J.M.P. van Trijp, M.N.C.P. Buysman, *Anal. Chem.* 68 (1996) 3511–3515.
- [21] M. Katyal, *Talanta* 15 (1968) 95–106.
- [22] B.S. Garg, R.P. Singh, *Talanta* 18 (1971) 761–766.
- [23] B.S. Garg, K.C. Tripathi, R.P. Singh, *Talanta* 16 (1969) 462–464.
- [24] G.W. Zhang, J.B. Guo, N. Zhao, J.R. Wang, *Sens. Actuators B* 144 (2010) 239–246.
- [25] M.Z. Si, R.G. Wu, P.X. Zhang, *Acta Photonica Sin.* 28 (1999) 839–840.
- [26] J. Sambrook, D. Russell, *Molecular Cloning: A Laboratory Manual*, third ed., Cold Spring Harbor Lab (CSHL) Press, New York, 2001.
- [27] J. Kang, Y. Liu, M.X. Xie, S. Li, M. Jiang, Y.D. Wang, *Biochim. Biophys. Acta* 1674 (2004) 205–214.
- [28] J.W. Kang, L. Zhuo, X.Q. Lu, H.D. Liu, M. Zhang, H.X. Wu, *Inorg. Biochem.* 98 (2004) 79–86.
- [29] C.X. Yang, Y.F. Li, P. Feng, C.Z. Huang, *Chin. J. Anal. Chem.* 30 (2002) 473–477.
- [30] J.Y. Bottero, J.M. Cases, F. Fiessinger, J.E. Poirier, *J. Phys. Chem.* 84 (1980) 2933–2939.
- [31] C.Z. Huang, K.A. Li, S.Y. Tong, *Anal. Chem.* 69 (1997) 514–520.
- [32] R.F. Pasternack, P.J. Collings, *Science* 269 (1995) 935–939.
- [33] H.P. Zhou, X. Wu, J.H. Yang, *Talanta* 78 (2009) 809–813.
- [34] Z.L. Zhang, W.M. Huang, J.L. Tang, E.K. Wang, S.J. Dong, *Biophys. Chem.* 97 (2002) 7–16.
- [35] Y.L. Zhou, Y.Z. Li, *Biophys. Chem.* 107 (2004) 273–281.
- [36] J.R. Lakowicz, *Anal. Biochem.* 324 (2004) 153–169.
- [37] I. Gryczynski, J. Malicka, Z. Gryczynski, J.R. Lakowicz, *Anal. Biochem.* 324 (2004) 170–182.